

Effects of the Cooling Path on Microstructure and Mechanical Properties of Vanadium-Microalloyed Forging Steel

KUN-YOU TSAI, HERNG-SHUOH JANG, YU-TING TSAI and LIN HSU

*Iron and Steel Research & Development Department
China Steel Corporation*

Vanadium microalloyed (VMA) forging steels can achieve their required high strength through vanadium carbide (VC)-precipitation strengthening during the cooling stages after hot forging, and consequently the traditional post forging heat treatments, such as normalizing, quenching and tempering, can be eliminated. Since precipitation of VC occurs in proeutectoid ferrite and ferrite lamellae of pearlite, the volume fraction of ferrite and the interlamellar spacing of pearlite also influence the strength of VMA forgings. In order to attain the desired mechanical properties, the forging process should be controlled to develop proper microstructure and VC precipitation, and the cooling path after forging is one of the most important parameters. In this study, 38MnVS6 was used to analyze the effect of reaction temperature on VC precipitation. By lowering reaction temperature, the VC particle size decreases, VC distribution density increases, and thus the strengthening effect is enhanced. The hot forging process was also simulated by Gleeble to investigate the effect of forging parameters on microstructure and mechanical properties. Soaking temperature, forging temperature and forging strain control the recrystallization and growth of austenite grains. Meanwhile, the cooling path determines the start and stop temperature of phase transformation and precipitation, as well as the microstructure and mechanical properties. Based on these results, the forging process could be modified and the performance of VMA forgings could be improved.

Keywords: Vanadium-microalloyed steel, Hot forging, Controlled coolings

1. INTRODUCTION

The benefit of the vanadium (V) addition to medium-carbon low-alloy forging steels has been recognized since the introduction of 49MnVS3, the first grade of vanadium microalloyed (VMA) forging steels, as a replacement for CK45 medium carbon quenched and tempered (QT) steel first introduced in Germany in 1972⁽¹⁾. In the past, a post-forging normalizing treatment was required for QT steel to homogenize the grain structure, enhance machinability, and minimize the distortion during the subsequent quenching process, and then quenching and tempering were applied to enhance strength and toughness. However, VMA steels could attain the same strength level and adequate toughness through appropriate alloy design and direct controlled cooling from the finishing-forging temperature. Due to the advantages of a shorter process, reduced distortion and lower cost, the development of VMA forging steels became increasingly popular in Europe, Japan and the USA. To date, VMA forging steels have been extensively used for automotive components or machinery parts.

VMA forging steels are strengthened by interphase

precipitation of vanadium carbide (VC). V can be fully dissolved during the preheating stage prior to forging because of its extensive solubility in austenite. In the following post-forging cooling stage, while ferrite and pearlite transformation occur, nanosized VC particles precipitate at austenite/ferrite interphase boundaries can provide significant strengthening for proeutectoid ferrite as well as ferrite lamellae of pearlite. The strength levels of VMA forgings could be simply selected through the linear relationship between V content and yield/tensile strength⁽²⁾. However, the actual performance of the forged product is also controlled by the forging process, in which the most critical parameters are preheating temperature, forging temperature, forging strain, and cooling path.

The preheating temperature is generally recommended at 1150°C -1250°C. Below this range may result in incomplete dissolution of the initial VC precipitates and reduce the strengthening capability, while above this range may cause excessive grain coarsening. The forging temperature and forging strain have little effect on the precipitation and strengthening contribution of VC, but it affects the recrystallization of austenite during and after each forging pass. Lowering the forging temperature

or increasing the forging strain could enhance the grain refinement of austenite and thus encourage the ferrite formation during the cooling stage, which leads to a slight decrease in strength but a significant improvement in ductility and toughness. The cooling path after forging is the most important parameter to control the microstructure and mechanical properties of the forged product since phase transformation and VC precipitation occur in this stage. In general, increasing the cooling rate decreases the phase transformation temperature, which is beneficial for precipitation strengthening due to the decrease in precipitate size and the increase in volume fraction. Moreover, faster cooling also results in a higher volume fraction and decreased interlamellar spacing of pearlite, which provides a further increase in the strength. However, when the cooling rate exceeds a critical value, undesired bainite transformation will take place and result in a significant degradation of toughness and ductility.

Although the metallurgical theory of VMA forging steels is well understood, there are still many variables and limitations that need to be considered in real practice. For example, the temperature and cooling rate will vary within a forging due to the variation in section size and the pass schedule. In some cases, two-step cooling is required to avoid unfavorable microstructure and to attain better mechanical properties. In order to stably control the performance of forged product under various conditions, a comprehensive investigation of the effect of the cooling path on the microstructure and mechanical properties is necessary. In this study, grade 38MnVS6, a popular VMA steel for general use in the automotive industry, was selected for this research. The effect of transformation temperature on the precipitation of VC is analyzed, and the forging and cooling process is simulated by Gleeble to investigate the variations in microstructure and hardness.

2. EXPERIMENTAL METHOD

The materials tested were obtained from commercial 38MnVS6 steel rods with a composition specification given in Table 1 according to European standard EN 10267. All the specimens were taken from the mid-radius location to prevent possible defects. Isothermal heat treatment was selected to study the effect of transformation temperature on the precipitation of VC. Specimens were austenitized at 1150°C for 30 minutes and

subsequently treated in a salt bath at 600°C to 650°C for 30 minutes, followed by a water quench. The yield strengths of treated specimens were measured by standard tensile tests, and the microstructure was characterized by optical and transmission electron microscopies. The OM samples were prepared using standard metallographic techniques and etched by 3% nital solution. Ferrite fractions in the optical micrographs were quantified by image analysis software (Image J). TEM thin foil specimens were prepared by twin-jet electropolishing machine and observed with JEOL JEM-2100Plus. Particle size and number of unit area of VC were measured directly from TEM images, while particle densities were estimated with the aid of local foil thickness which were determined by the convergent beam electron diffraction (CBED) technique⁽³⁾.

The forging and controlled cooling processes were simulated by uniaxial hot compression test in GLEEBLE 3800. Cylindrical specimens with a diameter of $\phi 10$ mm and a height of 15mm were machined in the rolling direction. Figure 1 shows a schematic of the simulation process and the parameters controlled in this study. The preheating temperature (T_{PH}), forging temperature (T_{FG}), and compression strain (ϵ) were chosen to observe the effect of prior-austenite microstructure. One- or two-step cooling paths were executed to analyze the effect of cooling rate (CR_1/CR_2) and transition temperature (T_S). The tested specimens were sectioned along the compression axis and prepared for OM observation as above methods. Vickers hardness was also measured using a load of 2 kgf. The microstructure observation and hardness testing were carried out at the center of the section.

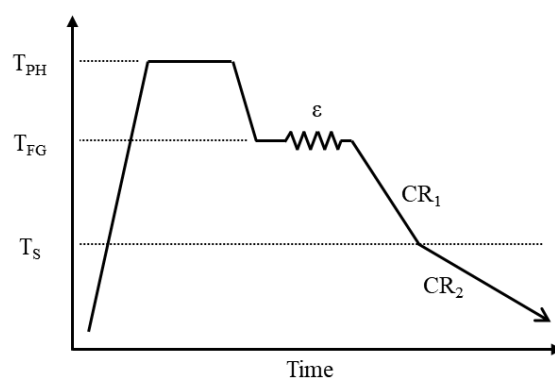


Fig.1. Schematic diagram of the Gleeble simulation process.

Table 1 Chemical composition of 38MnVS6 according to European standard EN 10267.

wt%	C	Si	Mn	P	S	Cr	Mo	V	N	Al, Ti...
Min.	0.34	0.15	1.20	--	0.020	--	--	0.08	0.010	cust.
Max.	0.41	0.80	1.60	0.025	0.060	0.30	0.08	0.20	0.020	

3. RESULTS AND DISCUSSION

3.1 Effect of Transformation Temperature

Figure 2 (a) and 2 (b) show the microstructure of 38MnVS6 samples isothermally transformed at 600°C and 650°C, respectively. Both conditions result in a similar microstructure consisted of proeutectoid ferrite and pearlite. However, the grain size of proeutectoid ferrite increases with the transformation temperature, and the ferrite fraction also increase from 11% to 18%. In TEM observation, the sheet-like characteristic of interphase precipitation could only be seen under the tilting condition that the incident electron beam is parallel to the sheet planes. Figure 3 (a) and 3 (b) show the representative TEM micrographs of proeutectoid ferrite and pearlite transformed at 600°C, respectively. Rows of VC particles can be seen in proeutectoid ferrite and ferrite lamellae of pearlite. The selected area diffraction patterns show that Figure 3 (a) and 3 (b) are taken from different zone axes (αFe [001] and αFe [012], respectively), however, the orientations of the sheet planes in both figures are close to αFe (200) plane.

The mean precipitate size (d) and mean inter-sheet spacing (h) were measured through TEM images. The mean inter-particle spacing (w) was estimated by CBED

technique. Thus, the volume fraction of precipitates $f = 1/hw^2$ was obtained. It has been well known that refining the particle dispersion leads to higher strengthening effect. According to Ashby-Orowan relationship^(4,5), the increase in yield strength contributed by the interphase precipitation is given as

$$\Delta\sigma_{pre} = 0.504 \frac{Gb f^{0.5}}{d(1-2(f/\pi)^{0.5})} \ln \frac{kd}{2.45b} \dots\dots\dots(1)$$

where G is the shear modulus, b is the Burgers vector, k is a constant estimated as 1 for VC in pearlite, and as 2.7 in ferrite. These measured or estimated results are shown in Table 2. At the same transformation temperature, the precipitate size, inter-sheet and inter-particle spacing in pearlitic ferrite are smaller than those in proeutectoid ferrite. Furthermore, lowering the transformation temperature leads to smaller precipitate size, inter-sheet and inter-particle spacing. Although the VC precipitation in pearlitic ferrite is finer and denser than that in proeutectoid ferrite, the calculated $\Delta\sigma_{pre}$ for pearlite is lower since the strengthening only occurs in the ferrite lamellae of pearlite. Nevertheless, the calculated $\Delta\sigma_{pre}$ for both pearlite and proeutectoid ferrite increase by 11~32 MPa while the transformation temperature decreases from 650°C to 600°C.

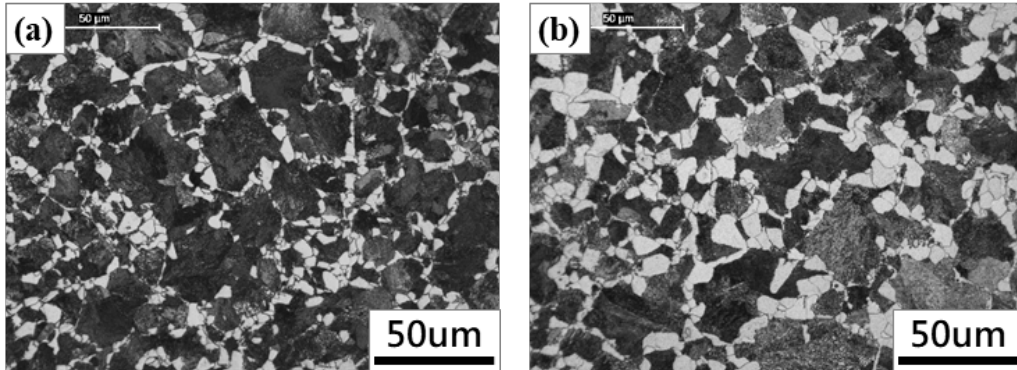


Fig.2. Optical metallographs of specimens isothermally treated at (a) 600°C and (b) 650°C.

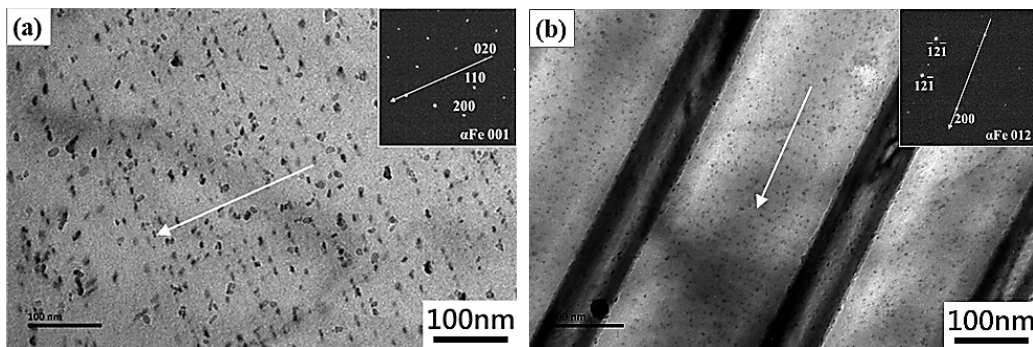


Fig.3. TEM images taken from (a) ferrite and (b) pearlite of specimens isothermally treated at 600°C.

The experimental results of yield strength are also listed in Table 2. According to Gladman's theory⁽⁶⁾, the yield strength of ferrite-pearlite steels can be described as

$$\sigma_{YS} = X_F^n \sigma_F + (1 - X_F^n) \cdot \sigma_P \dots \dots \dots (2)$$

where X is volume fraction, n is empirically fitted as $1/3$, and the lower indexes ' F ' and ' P ' represent ferrite and pearlite, respectively. Based on the relationship of equation (2), the overall contributions of precipitation strengthening in these isothermally treated specimens were estimated to be about 26% of the yield strengths, as shown in Table 2. Moreover, the increases in calculated $\Delta\sigma_{pre}$ due to the decrease in transformation temperature are significantly lower than the increase in yield strength (more than 100 MPa). It is because that the transformation temperature affects not only precipitation reaction, but also grain size, ferrite volume fraction, and interlamellar spacing of pearlite.

3.2 Effect of Forging Parameters

In the forging stage the steels are processed within the temperature range of austenite, and therefore the most important phenomena in this stage are recrystallization and grain growth. To study the effect of forging parameters on these phenomena, the key parameters controlled in Gleeble simulations are T_{PH} , T_{FG} , and ϵ , while the cooling paths ($CR_1=2.5^\circ\text{C}/\text{s}$, $CR_2=0.5^\circ\text{C}/\text{s}$, $TS=650^\circ\text{C}$) are fixed for comparison.

Figure 4 (a) to 4 (d) show the effect of T_{PH} on the microstructure. The prior-austenite grain boundary can be identified by the distribution of proeutectoid ferrite. When $T_{PH}=900^\circ\text{C} \sim 1200^\circ\text{C}$, the microstructures are equiaxed fine grain which mean that full recrystallization occurred during the forging process. Meanwhile, the prior-austenite grain size increases with T_{PH} . It is because that the initial grain size before deformation is determined mostly in the reheating stage, and the recrystallized grain size increases with the initial grain size.

Table 2 Data of VC precipitates, precipitation strengthening, and yield strength from the specimens isothermally treated at 600°C and 650°C . (Units: d, h, w: nm; $\Delta\sigma_{pre}$, YS: MPa)

Temp.	Ferrite				Pearlite				Overall $\Delta\sigma_{pre}$	Exp. YS
	d	h	w	$\Delta\sigma_{pre}$	d	h	w	$\Delta\sigma_{pre}$		
600°C	4.0	16.0	33.7	222.9	3.5	11.6	27.7	126.4	172.5	687.1
650°C	5.0	20.8	47.5	190.6	4.0	16.8	33.2	115.9	158.2	581.1

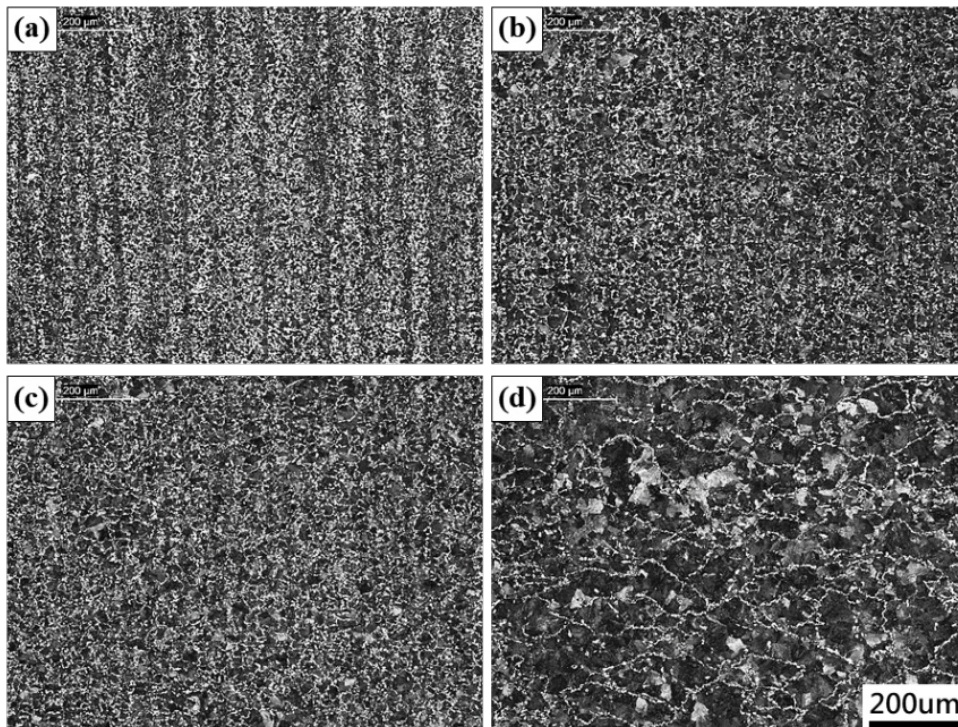


Fig.4. Metallographs of Gleeble simulated specimens. $T_{PH}=(a) 900^\circ\text{C}$; (b) 1100°C ; (c) 1200°C ; (d) 1280°C .

However, when $T_{PH}=1280^{\circ}\text{C}$, the pancake-type microstructure indicates that the deformed austenite grains did not recrystallize, and the prior-austenite grain size is significantly larger than the others. According to the recrystallization theory, there is a critical strain (ϵ_C) required to induce the nucleation process. Since the strain energy comes from the accumulation of dislocations on grain boundaries, increasing in grain size results in fewer grain boundaries and less local strain to trigger nucleation. Moreover, higher T_{PH} leads to less ferrite volume fraction and higher hardness as shown in Figure 5. However, an over coarsened grain structure is harmful to toughness and fatigue resistance and should be avoided.

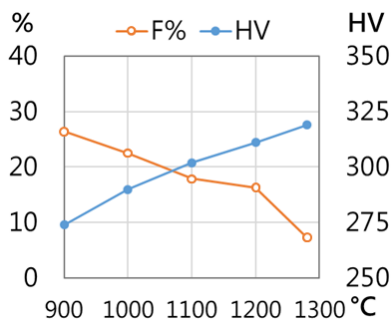


Fig.5. Variations in ferrite fraction and hardness as a function of T_{PH} .

Figure 6(a) shows the variations in microstructure with different T_{FG} and ϵ , and the initial grain sizes are controlled by the same preheating process ($T_{PH} = 1200^{\circ}\text{C}$). In general, higher T_{FG} enhances the growth of

prior-austenite grains, and in contrast, higher ϵ enhances grain refinement. However, when $\epsilon < \epsilon_C$, the strain energy becomes the excess driving force for grain coarsening, and even causes abnormal grain growth (AGG). The metallograph with $\epsilon=0.05$ and $T_{FG}=1200^{\circ}\text{C}$ shows an example of strain-induced grain coarsening, while that with $\epsilon=0.05$ and $T_{FG}=900^{\circ}\text{C}$ shows a duplex grain structure (AGG) due to insufficient thermal energy for extensive grain growth.

In order to further reveal the influence of small strain ($< \epsilon_C$) on the development of grain structure, a two-pass deformation scheme was applied, in which a large strain ($\epsilon=0.35$) was introduced at 1100°C and held for 5 sec to ensure full recrystallization, and followed by a small strain ($\epsilon=0.05$) at 1100°C or 1000°C to induce AGG. As shown in Figure 6(b), grain growth only occurs sporadically at the center of the specimen when a small strain was applied at 1000°C . In contrast, when the small strain was applied at 1100°C , the region of coarsened grains almost extends to the full cross-section. The results clearly show the effect of thermal energy and strain energy on the kinetics of grain growth.

3.3 Effect of the Cooling Path

In this section, the forging processes were fixed ($T_{PH}=1200^{\circ}\text{C}$, $T_{FG}=1000^{\circ}\text{C}$, and $\epsilon=1$) and followed by variant cooling paths to study their effects on microstructure and mechanical properties. Firstly, constant cooling rates ($CR_1=CR_2$) were used, and the variations in phase fraction and hardness as a function of cooling rate are shown as Figure 7(a). The results show a recommended CR window of $0.5^{\circ}\text{C/s} \sim 1^{\circ}\text{C/s}$. A too slow CR may cause insufficient hardness due to a high volume

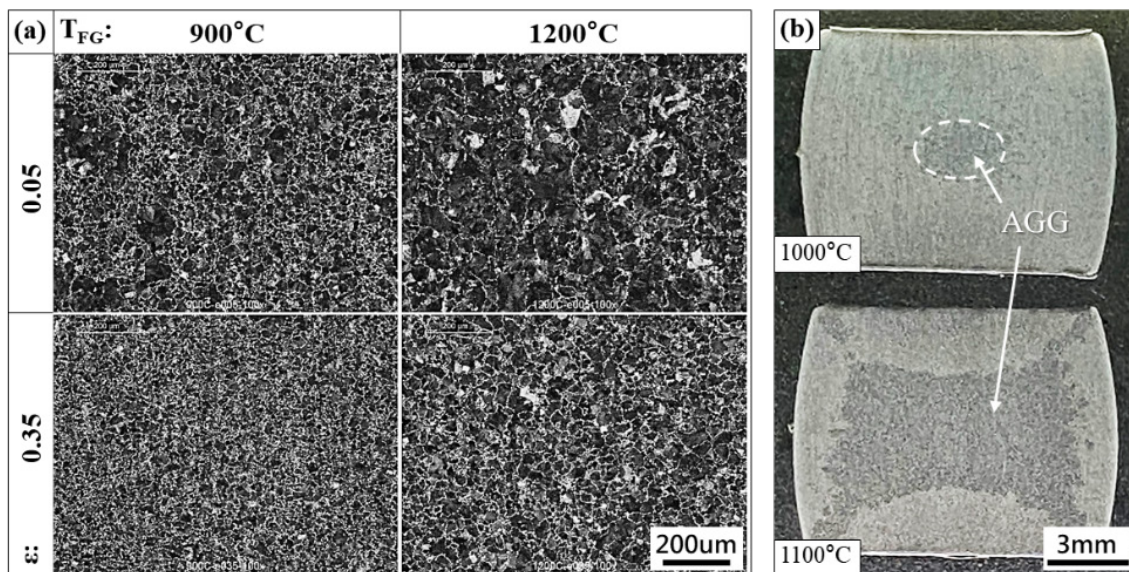


Fig.6. (a) Variations of microstructure with different T_{FG} and ϵ ; (b) cross-sections of the two-pass deformed specimens.

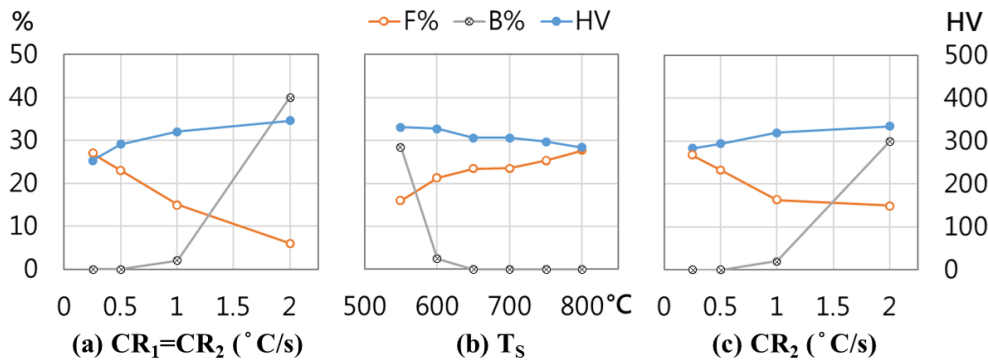


Fig.7. Variations in phase fraction and hardness as a function of (a) $CR_1(=CR_2)$; (b) T_s ; (c) CR_2 .

fraction of ferrite (F%), coarse pearlite and precipitation transformed at a higher temperature. Conversely, a too fast CR may cause the formation of undesired bainite.

In order to obtain higher strength and avoid the formation of bainite, a two-stage cooling method is recommended⁽¹⁾, in which a fast-cooling stage (CR_1) is applied from finishing-forging temperature to transition temperature (T_s) to lower the transformation temperature, and followed by a slow cooling stage (CR_2) to ensure the ferrite-pearlite transformation is completed. In general, the phase transformation occurs mainly in the second stage, and the experimental results (not shown here) reveal that CR_1 has no significant effect on microstructure and hardness unless $CR_1 < 0.5^\circ\text{C/s}$. Figure 7(b) and 7(c) show the variations in phase fraction and hardness as a function of T_s and CR_2 , respectively. It can be seen that when lowering T_s or increasing CR_2 , F% decreases and hardness increases. However, bainite fraction (B%) increases when $T_s < 600^\circ\text{C}$ or $CR_2 > 1^\circ\text{C/s}$, and these values can be seen as the critical condition of two-stage cooling.

4. CONCLUSION

In this study, the precipitation strengthening of 38MnVS6 vanadium-microalloyed forging steel was analyzed through isothermal heat treatment and TEM. The effect of forging parameters and cooling paths on the microstructure and mechanical properties of 38MnVS6 was also investigated by Gleeble simulation. The obtained results are summarized as follows.

1. Lowering the transformation temperature leads to the refinement of interphase precipitation of VC and thus the enhancement of precipitation strengthening.
2. The contribution of VC precipitation strengthening $\Delta\sigma_{pre}$ is about 26% of YS. When the transformation temperature decreases from 650°C to 600°C , the increase in $\Delta\sigma_{pre}$ is about 13.5% of the increase in YS, and the remaining comes from the decrease in ferrite volume fraction and the refinement of ferrite grain

size and interlamellar spacing of pearlite.

3. Forging parameters control the development of austenite grain structure, while cooling paths control the ferrite-pearlite transformation and the precipitation of VC.
4. Higher preheating temperature and forging temperature lead to coarser prior-austenite grain size due to the thermal activated grain growth. In contrast, higher forging strain enhances grain refinement due to the recrystallization of austenite.
5. However, when the forging strain is insufficient to activate recrystallization, the strain energy becomes the excess driving force for grain coarsening and may induce abnormal grain growth.
6. Two-stage cooling method is favorable to obtain higher strength and avoid the formation of bainite. In the first stage a fast cooling rate ($>0.5^\circ\text{C/s}$) is recommended to lowering the transformation temperature, and a transition temperature higher than 600°C and a cooling rate lower than 1°C/s in the second stage are required to avoid the formation of undesired bainite.

REFERENCES

1. Y. Li and D. J. Milbourn: "Vanadium Microalloyed Forging Steel"; pp. 47-54 in Proc. of the 2nd Int. Symposium on Automobile Steel, Anshan, China, 2013.
2. J. F. Held: "Some Factors Influence the Mechanical Properties of Microalloyed Steel"; pp. 175-188 in Conf. Proc. Fund. Microalloying Forging Steels, Colorado, USA, Jul. pp. 8-10, 1986.
3. S. M. Allen: Phil. Mag. A, 1981, v.43, pp. 325.
4. H. H. Kuo, M. Umemoto, K. Sugita, G. Miyamoto and T. Furuha: ISIJ Int., 2012, v.52, n.4, pp. 669.
5. T. Gladman: Mater. Sci. Tech., 1999, v.15, n.1, pp. 30.
6. T. Gladman, I. D. Mcivor and F. B. Pickering: J. Iron Steel Inst., 1972, v.12, pp. 916.